Vrije Universiteit Brussel

Evaluation of Failure Trends on a PID-Controlled Synchronous Buck Converter based Battery Charging Controller

Hasan, Mohammed Mahedi; Hasan, Md. Mahamudul; Chakraborty, Sajib; El Baghdadi, Mohamed; Razzak, Md. Abdur; Hegazy, Omar

Published in:
Evaluation of Failure Trends on a PID-Controlled Synchronous Buck Converter based Battery Charging Controller

DOI:
10.1109/PESGRE45664.2020.9070671

Publication date:
2020

Document Version:
Proof

Link to publication

Citation for published version (APA):
Hasan, M. M., Hasan, M. M., Chakraborty, S., El Baghdadi, M., Razzak, M. A., & Hegazy, O. (2020). Evaluation of Failure Trends on a PID-Controlled Synchronous Buck Converter based Battery Charging Controller. In *Evaluation of Failure Trends on a PID-Controlled Synchronous Buck Converter based Battery Charging Controller* (pp. 1-6). [9070671] (2020 IEEE International Conference on Power Electronics, Smart Grid and Renewable Energy, PESGRE 2020). https://doi.org/10.1109/PESGRE45664.2020.9070671

General rights
Copyright and moral rights for the publications made accessible in the public portal are retained by the authors and/or other copyright owners and it is a condition of accessing publications that users recognise and abide by the legal requirements associated with these rights.

- Users may download and print one copy of any publication from the public portal for the purpose of private study or research.
- You may not further distribute the material or use it for any profit-making activity or commercial gain
- You may freely distribute the URL identifying the publication in the public portal

Take down policy
If you believe that this document breaches copyright please contact us providing details, and we will remove access to the work immediately and investigate your claim.

Download date: 29. Nov. 2021

Evaluation of Failure Trends on a PID-Controlled Synchronous Buck Converter based Battery Charging Controller

Mohammed Mahedi Hasan[1, 2], Md. Mahamudul Hasan[3], Sajib Chakraborty[1, 2], Mohamed El Baghdadi[1,2], Md. Abdur Razzak[3] and Omar Hegazy[1, 2]*

[1]*Vrije Universiteit Brussel (VUB), ETEC Department and MOBI Research Group, Pleinlaan 2, 1050 Brussels, Belgium*

[2]*Flanders Make, 3001 Heverlee, Belgium*

[3]*Independent University, Bangladesh, Department of EEE, Plot-16, Block-B, Bashundhara, Dhaka-1229, Bangladesh*

*Correspondence: omar.hegazy@vub.be

***Abstract*— The future trends in renewable energy generation are to select appropriate components and topology for power electronics converters with optimized costs and power density while satisfying the reliability target. This paper evaluates the reliability of a PID-controlled synchronous buck converter-based (SBC) battery charging controller for solar-powered lighting system in a fishing trawler and figure out most failure prone components. This reliability prediction has been developed according to MIL-HDBK-217F(N1/2) handbook models along with performance degradation analysis of individual components. Simulation results have demonstrated that that there are two general failure effects of components in the overall circuit, with the MOSFETs being the most failure prone device for a wide range of temperature; however, the overall system can expect an average operational lifetime of between 5 to 11 years before failing, under worst case scenario.**

Keywords—Power losses, junction temperature, MTBF, converter, reliability.

I. INTRODUCTION

One of the key challenges for transitioning from a fossil fuel-based energy economy to a renewable energy-based economy is the reliability of the power electronic components involved in the energy extraction and storage process. Power density, efficiency, cost, and reliability are the major concerns when designing any power electronic system [1], especially so in marine systems, where the operating conditions are very harsh. This paper will look at the reliability of the PID controlled SBC-based battery charging controller designed for a solar-power lighting system in a fishing trawler operating in the Bay of Bengal.

Reliability, which is defined as the probability that a product will continue to work for a specified time interval under specific conditions, is a key element of the product life cycle analysis (LCA) [2]. The traditional model to ensure reliability of a product relied on extensive testing of the product during the manufacturing phase (alpha), and on the consumer to find faults within the final product during normal use (beta). Consistent and reproducible faults are then identified and analyzed before a fix or a solution to the fault is released. To a large extent, when the product is a software, that is still the case. While, reliability in modern hardware-based system is ensured with Design for Reliability (*DfR*), a design process for ensuring that the product performs its specified function, over its expected lifetime, within its use environment [3]. It is an iterative process that typically consists of six stages that span the product's lifecycle from concept till retirement: requirements definition, risks identification, reliability design, analysis and assessment, verification, validation or demonstration, and monitor or control [4].

This paper presents a model to describe the overall reliability of the SBC system used for the battery charging controller in a fishing trawler. To investigate the reliability of the converter, the components configurations, components ratings and system rating are taken as input for reliability evaluation. The thermal stresses on each component is obtained from electro-thermal model also consider as input. Afterwards the data gathered from the military handbook, MIL-HDBK-217F(N1/2), to identify the component failure rates, which will be used to predict the system level reliability of the SBC as shown in Fig. 1.

The paper is organized as follows: Section II will describe the physics of loss for the system based mainly on the thermal model of the SBC, Section III will perform a reliability analysis of the system, with Section IV analyzing the results, followed by a concluding section.

II. SYSTEM MODELING AND INSTANTANEOUS POWER LOSSES PROFILE

The trawler in question is one of hundreds of medium sized boats that ply the waters off the coast of Chittagong in the Bay of Bengal. These trawlers, which originally had diesel generators to power the electrical system on board the trawler, were modified to incorporate solar energy as the electrical source. Therefore, a 120W solar panel, a 1.2kWh lead acid battery, and a charging unit was incorporated. The charge controller is based on a synchronous buck controller that utilized a PID algorithm (instead of the traditional MPPT algorithm) to charge the battery using maximum available current. While the life cycle analysis (LCA) of the system was performed in [5] and its control structure and performance were extensively evaluated in [6], this paper will conclude the investigation with an analysis of the system reliability.

As reliability of a semiconductor-based system is highly influenced by temperature effects, thermal stress due to instantaneous power losses needs to be analyzed. As per mode operation of SBC, the losses in the SBC's power switches can be defined as [7, 8]:

$$P_{loss\_semi} = P_{Q1} + P_{Q2} + P_{BD} \quad (1)$$

XXX-X-XXXX-XXXX-X/XX/$XX.00 ©20XX IEEE

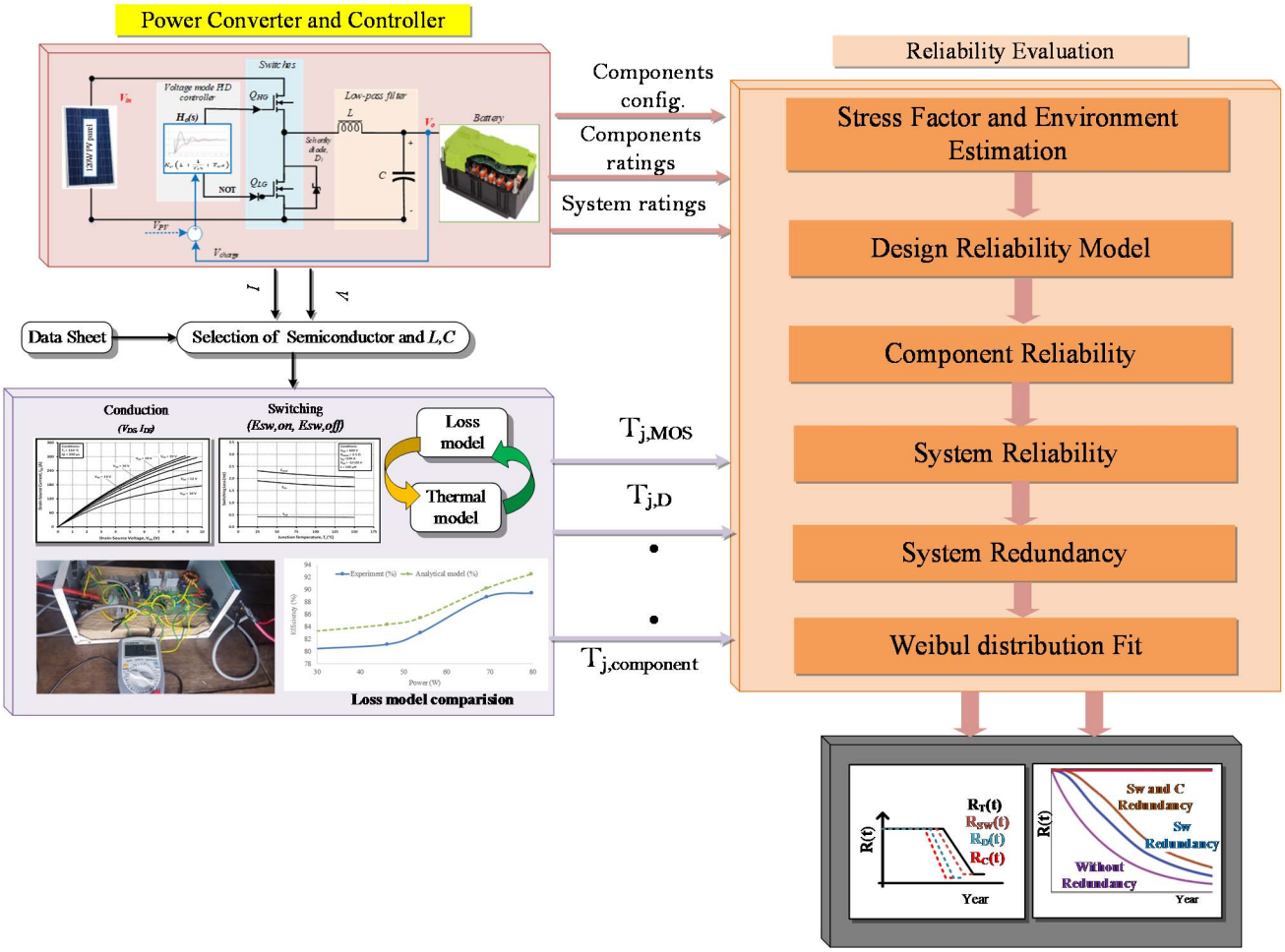

Fig. 1. Reliability analysis methodology of the Synchronous Buck Converter.

where P_{Q1} is the total power losses in upper switch, P_{Q2} is the total power losses in lower switch, and P_{BD} is the body diode losses. The total power losses in the upper switch are composed of conduction losses (P_{C1}), switching power losses (P_{SW}), and gate drive losses (P_G). Thus, the total losses are:

$$P_{Q1} = P_{C1} + P_{SW} + P_G \tag{2}$$

On the other hand, the switching losses for lower switch can be ignored. Typically, the lower side switch is conduction loss dominated with additional diode conduction losses for dead times. Therefore, the total loss in lower switch is comprised of conduction losses (P_{C2}) and gate drive losses (P_G) [5, 6].

$$P_{Q2} = P_{C2} + P_G \tag{3}$$

The conduction losses are:

$$P_{C1} = \left(I_{s,rms}D\right)^2 \times R_{DS(on)} \tag{4}$$

$$P_{C2} = [I_{s,rms}(1-D)]^2 \times R_{DS(on)} \tag{5}$$

The switching losses are:

$$P_{SW} = \frac{[V_{DS(max)}(t_r + . t_f).I_{s,rms}]f_{sw}}{2} \tag{6}$$

The gate-drive losses are:

$$P_G = V_{GS} \cdot \frac{Q_{gs}}{t_{on}} \cdot f_{sw} \tag{7}$$

The body diode losses are:

$$P_{BD} = 2 \cdot V_f \cdot \left(I_O + \frac{\Delta I_L}{2}\right) \cdot t_d \cdot f_{sw} \tag{8}$$

where the MOSFET parameters ($R_{DS(on)}$, $V_{DS(max)}$, t_r, t_f, V_{GS}, Q_g, t_{on}, V_f and t_d) are taken from the FQP50N60 datasheet. I_o, $I_{s,rms}$, and ΔI_L are the output current, switch current, and input current ripples, respectively. The inductor losses are the sum of core losses in the iron-powered toroidal core (P_{core}) and conducting losses in the windings of the inductor (P_{cond}) [9].

$$P_{loss\_inductor} = P_{Core} + P_{Cond} \tag{9}$$

with

$$P_{cond} = I_{L,rms}^2 R_L \tag{10}$$

$$P_{core} = W_t(f_{sw}^{1.68} B_{ac}^{1.99}) \tag{11}$$

and

$$B_{ac} = \frac{L\Delta I_L}{N_t} \tag{12}$$

where B_{ac} =magnetic flux density ripple, R_L = internal resistance of the coil, W_t = weight of the inductor, L = core-length, and N_t = number of turns.

The ESR losses of DC link capacitor can be calculated as:

$$P_{loss\_C} = I_{c,rms}^2 ESR \tag{13}$$

The total losses of the system then are the sum of all losses of all components in the SBC system.

$$P_{loss\_total} = P_{loss\_semi} + P_{loss\_inductor} + P_{loss\_capacitor} \quad (14)$$

Based on the power loss model, the RC lumped equations have been developed to predict the junction temperature (T_j) and heat sink temperature (T_H) as equation (15) and (16) [11].

$$T_j = T_a + P_{loss\_total}[Z_{th(jc)} + Z_{th(ch)} + Z_{th(ha)}] \quad (15)$$

$$T_H = T_a + P_{loss\_total} Z_{th(ha)} \quad (16)$$

where $Z_{th(jc)}$ is the junction-to-case thermal impedance (°C/W), $Z_{th(ch)}$ is the case-to-heatsink thermal impedance (°C/W), $Z_{th(ha)}$ is the heatsink-to-ambient thermal impedance (°C/W), and T_a is the ambient temperature.

The maximum Tj of the SBC during its operation will have a significant impact on selecting the range of operation to find component failure rates and thus will affect the reliability of the system.

III. System Reliability Evaluation

This section seeks to provide a prediction of the system Mean Time Between Failure (MTBF), to evaluate its potential reliability. This will provide information to assist in directing and planning for reliability and related program efforts, and to identify design features which are critical to reliability. The method of reliability prediction used in this analysis is taken from MIL-HDBK-217F(N1/2) [10]. The Mathematical Model used in determining the converter reliability is known as the series model. This model is based on the equation (17).

$$R(t) = e^{-\lambda t} = e^{-\frac{t}{MTBF}}, \because \lambda = \frac{1}{MTBF} \quad (17)$$

where $R(t)$ is the overall reliability of the converter, t is the elapsed operation time (hr), and λ is the constant failure rate.

The Reliability model MTBF reflects the reliability of all electrical parts in the topology. The component failure rates can be found using either the parts count method or the parts stress method. The difference between due is that the parts count method relies only on the generic failure rates of components to quickly determine an approximate reliability estimate, while the parts stress method is more operation specific. The part stress prediction model considers the component parameters and the stress factors for the components running and performing their intended function in their considered environment. The part stress prediction model is usually used after the design phase for reliability trade-offs vs part selection and stresses.

The quality of a part, which also play a vital role in its failure rate, for the converter has been selected as MIL Spec quality, but with a lower π_Q factor since they are sourced commercially. All part reliability model includes the effects of environment stresses through the environment factors, π_E. The Ground, Fixed type of environment has been selected for reliability model. Finally, a temperature analysis was done for each part ranging from ambient temperature (25°C) up to maximum Tj (105°C). The maximum range is fixed based on the thermal response of the SBC for rash mission profile. Table I summarizes the failure using the parts stress method for a worst-case scenario temperature of 105°C and average case scenario of 75°C, while Fig.2 shows the effect of temperature on failure rate for the three most vulnerable components (semiconductors such as MOSFET, MCU, and Diode).

As Table 1 shows, the overall part failure rate, λ_p, of the individual components depends on a combination of various stress factors including λ_b (base failure rate), π_T (temperature factor), π_Q (quality factor), π_A (application factor), π_E (environment factor), π_P (active pin factor), π_S (power stress factor), π_C (capacitance factor), π_V (voltage stress factor), π_{SR} (series resistance factor), C_1 (die complexity failure rate), C_2 (package failure rate), π_B (acceleration voltage breakdown), and π_L (learning factor). The right sign (✓) represents the stress factor applying to the components. The temperature factor, π_T, in turn depends on the temperature of the component, Tj, and the temperature coefficient, Ea based on the Arrhenius equation. The likelihood of systems failing due to failure in passive devices such as inductors, resistors, and capacitors are negligible. Thus, major reliability system models are based on the reliability of the semiconductor components (Diode, MOSFET, Microcontroller).

To calculate the overall reliability of the system, it is necessary to ascertain system functionality in the face of failures to individual or groups of components. Simulations of the system in Simulink were used to investigate how a system reacts to failure in individual components. A component can fail in many ways, but the effect of that failure on an electrical circuit can often be felt as an “open circuit” or a “short circuit” where the component is located. Simulations show that open circuit or short circuit failure in the inductor causes total system failure. Open circuit failure in the capacitor allow the system to operate, albeit with higher THD in the output, whereas short circuit failure of the capacitor cause total system failure. In the SBC, there are two MOSFET/diode components in the circuit, one connected in series, while the other is connected in parallel. Considering the parallel MOSFET/diode component, if the MOSFET or diode suffer an open circuit failure, the other component provides redundancy, and the system operates properly, albeit with low efficiency. On the other hand, if the MOSFET or diode suffers from a short circuit failure, it causes total system failure. Finally, considering the series MOSFET/diode component, if the MOSFET or diode suffers from a short circuit failure or the MOSFET suffers from an open circuit failure, it causes total system failure. However, if the diode suffers from an open circuit failure, it has no effect on the system. The microcontroller unit (MCU) is an interesting case since its failure manifest in the circuit as two invalid control inputs: both control inputs are continuously low or continuously high.

Table 1:Failure rates of the individual components of the Synchronous Buck Converter at 105°C

Component Name	Failure rate (λ_p)	Stress Factors	Quantity (N)
Resistor	8.72 * 10^{-2}	$\lambda_p = \lambda_b\pi_T\pi_P\pi_Q\pi_S\pi_E$ where λ_b = 0.0024, Ea = 0.08, π_P = 0.58, π_Q = 10, π_S = 0.81, and π_E = 4	1
Inductor	1.337 * 10^{-3}	$\lambda_p = \lambda_b\pi_T\pi_Q\pi_E$ where λ_b = 0.00003, Ea = 0.11, π_Q = 3, and π_E = 6	1
MOSFET	16.5	$\lambda_p = \lambda_b\pi_T\pi_Q\pi_E\pi_A\pi_B$ where λ_b = 0.012, Ea = 0.166, π_Q = 5.5, π_E = 6, π_A = 8, and π_B = 1.33	2
MCU	2.776	$\lambda_p = (C_1\pi_T+C_2\pi_E)\pi_Q\pi_L$ where C1 = 0.14, C2 = 0.024, Ea = 0.06, π_E = 2, π_Q = 10, and π_L = 1	1
Capacitor	1.258	$\lambda_p = \lambda_b\pi_T\pi_P\pi_Q\pi_S\pi_E$ where λ_b = 0.00037, Ea = 0.35, π_P = 1.9, π_Q = 10, π_S = 1, and π_E = 10	1
Diode	1.778	$\lambda_p = \lambda_b\pi_T\pi_Q\pi_S\pi_E\pi_C$ where λ_b = 0.003, Ea = 0.266, π_Q = 5.5, π_S = 1, π_C = 2, and π_E = 6	2
Connectors and sockets	5.669 * 10^{-2}	$\lambda_p = \lambda_b\pi_T\pi_P\pi_Q\pi_E$ where λ_b= 0.00064, Ea = 0.35, π_P = 5.5, π_Q = 0.3, and π_E = 3	2
Fuse	2 * 10^{-2}	$\lambda_P = \lambda_b\pi_E$ where λ_b = 0.02 and π_E = 1	1

where $\pi_T = e^{-\frac{Ea}{k}*\left(\frac{1}{Tj+273}-\frac{1}{298}\right)}$ and k = 8.6173303 * 10^{-5}. The other factors are constants specific to the component.

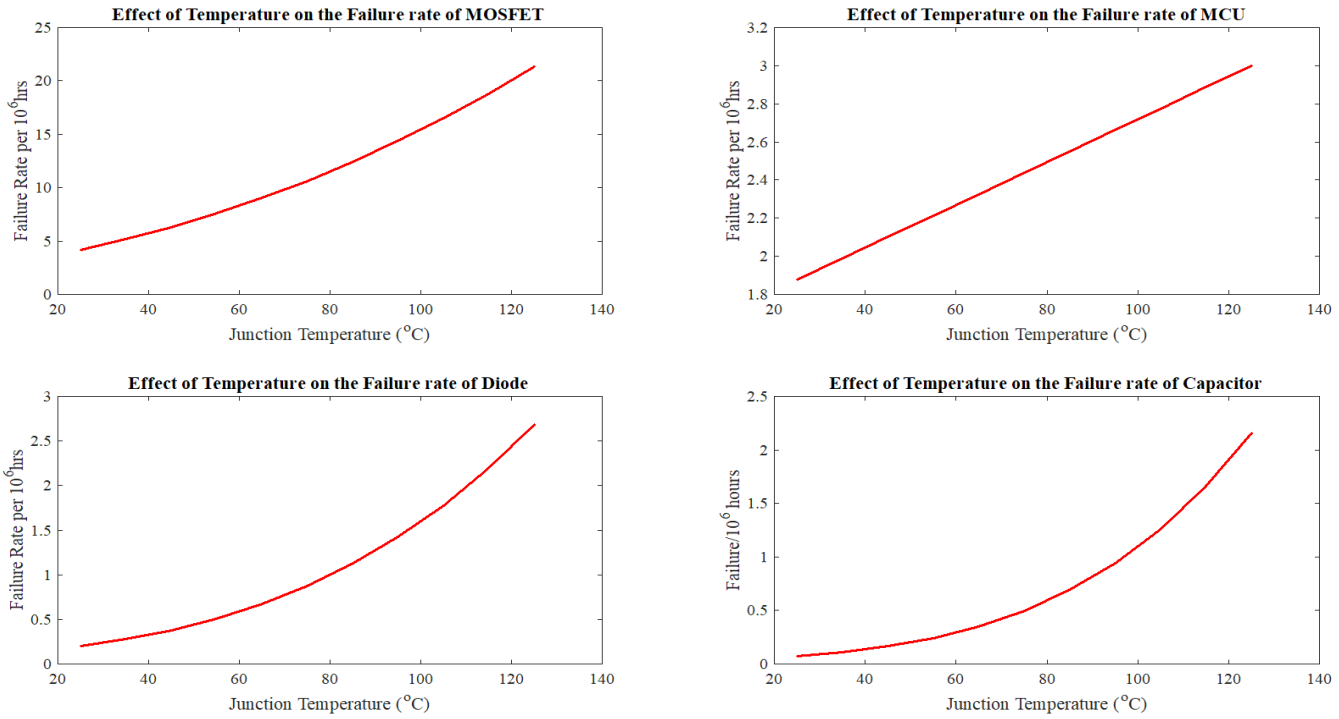

Fig. 2. Effect of temperature on failure rates of the four most failure prone components in the SBC

Both MCU failure combinations of the control inputs cause system failure. To summarize, the following causes total system failure: any type of failure in the inductor, short circuit failure of the capacitor, short circuit failure of the parallel connected MOSFET or Diode, any type of failure in the series connected MOSFET, short circuit failure in the series connected Diode, and any type of failure of the MCU control inputs. For all components, half of the value of the failure rate from Table I is used for calculations, assuming every component has equal chance to fail as either a short circuit or an open circuit. Moreover, two different reliability scenarios will be investigated, one where the components fail as a short circuit, and the other when they fail as an open circuit. Based on the methodology described in [11] and [12], the parallel connected MOSFET/diode components are modelled as parallel association if they fail as an open circuit, because the system fails only if both devices fail, while they are modelled as a series association if they fail as a short circuit, because the system will fail if any of the components fails. The remaining components of the SBC are modelled as series association, but in the case of open circuit failure, the capacitor and the series diode are not considered as their failure do not affect the system.

Reliability calculation for Series Association is given as follows:

$$R(t) = \prod_{i=1}^{n} R(t)_i = e^{-n\lambda t} \quad (18)$$

$$\lambda = \sum_{i=1}^{n} \lambda_i \quad (19)$$

$$MTBF = \frac{1}{\sum_{i=1}^{n} \lambda_i} \quad (20)$$

Reliability calculation for Parallel Association can be expressed as:

$$(1 - R(t)) = \prod_{i=1}^{n} (1 - R(t)_i) \quad (21)$$

$$R(t) = 1 - (1 - e^{-\lambda t})^n \quad (22)$$

$$MTBF = \frac{1}{\lambda} \sum_{i=1}^{n} \frac{1}{i} \quad (23)$$

Based on (18) and (21), and the description given above, the equations for the two types of failure scenarios are given as:

$$R_{SC}(t) = e^{-\frac{8.252t}{1000000}} \cdot e^{-\frac{0.889t}{1000000}} \cdot e^{-\frac{8.252t}{1000000}} \cdot e^{-\frac{0.889t}{1000000}} \cdot e^{-\frac{1.388t}{1000000}} \cdot e^{-\frac{0.629t}{1000000}} \cdot e^{-\frac{0.000668t}{1000000}} = e^{-\frac{20.299t}{1000000}} \quad (24)$$

$$R_{OC}(t) = \left[1 - \left(1 - e^{-\frac{8.252t}{1000000}}\right) \cdot \left(1 - e^{-\frac{0.889t}{1000000}}\right)\right] \cdot e^{-\frac{8.252t}{1000000}} \cdot e^{-\frac{1.388t}{1000000}} \cdot e^{-\frac{0.000668t}{1000000}} = e^{-\frac{10.529t}{1000000}} \quad (25)$$

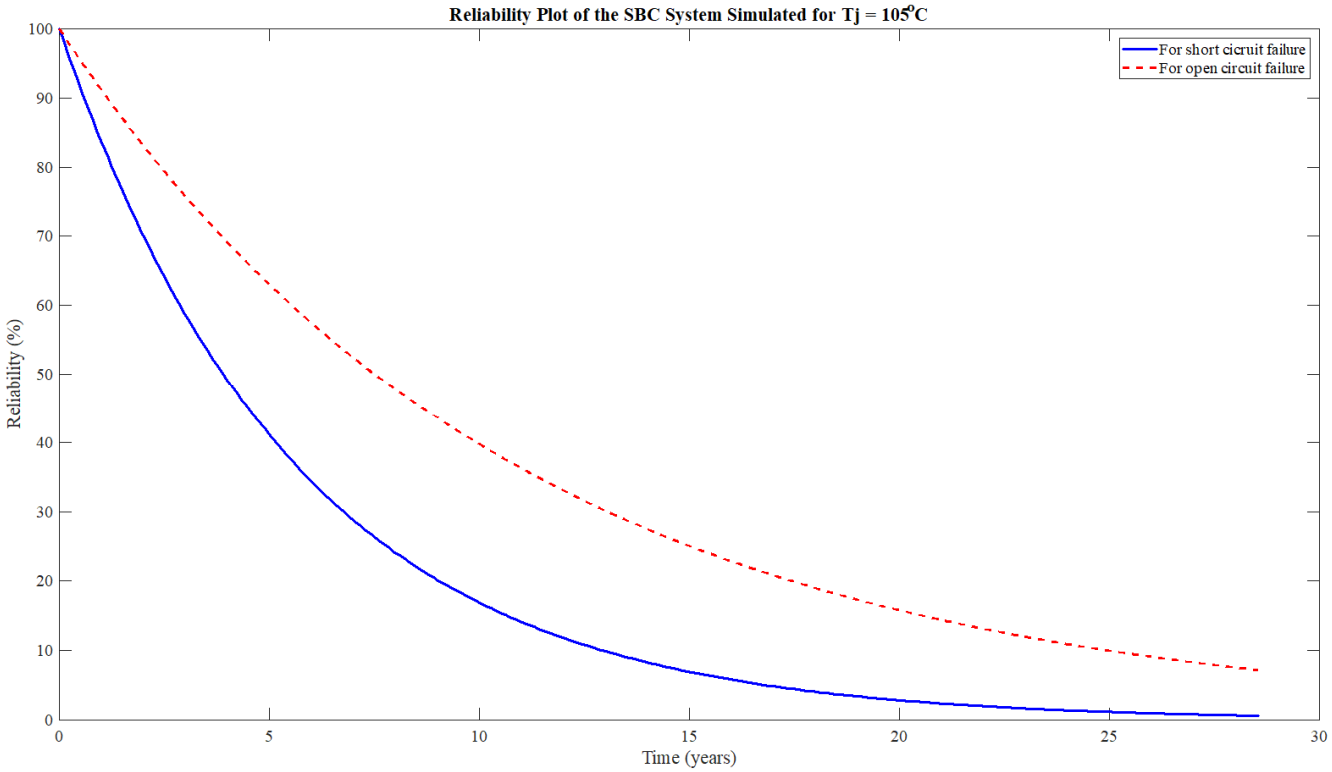

Fig. 3. System reliability of the SBC for Short and Open Circuit Failure conditions for Tj = 105°C

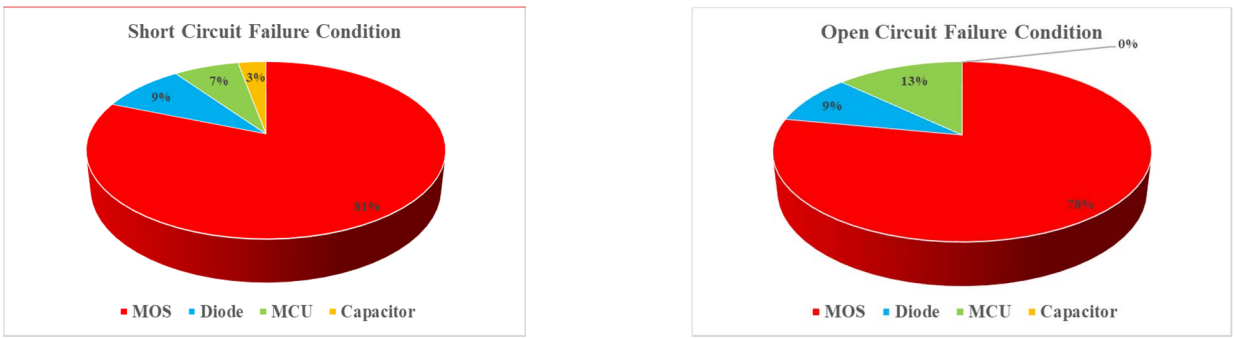

Fig. 4. Contribution of individual components in MTBF in Short and Open Circuit failure condition for Tj = 105°C

where ‘t’ is the time in hours. Reliability coefficients are given for Tj = 105°C. As can be seen, the system is twice more reliable (in the log scale) when experiencing open circuit failure than when experiencing short circuit failure. Also, the contribution of capacitor to the failure of the system disappears, while the contribution of the MCU doubles, but contributions of MOSFETS and Diodes remains unchanged.

IV. Results and Discussion

Fig. 4 represents the percentage of contributions of each component in MTBF and as expected MOSFET is the most failure prone component and contributes 81.3% of the failure rate for the Short Circuit failure scenario and 78.4% of the failure rate for the Open Circuit failure scenario.

Result 1 (worst case scenario): When operated at 105°C, the MTBF for the system is found to be between 5.62 to 10.84 years based on (24) and (25), and Fig. 3 shows that the system is mostly reliable for 3.88 to 7.42 years.

Result 2 (average case scenario): As comparison, the simulation was also run for operating temperature of 75°C, which is the junction temperature common in industrial applications. For the short circuit failure case, the system failure rate was found to be approximately 13 failures for every million hours of operation, which corresponds to a MTBF of 8.79 years, and the MOSFET was found to contribute to 81.92% of the failure. For the open circuit failure case, the system failure rate was found to be approximately 7 failures for every million hours of operation, which corresponds to a MTBF of 16.36 years, and the MOSFET was found to contribute to 76.23% of the failure. From this it can be concluded that the contribution of the MOSFET to the overall failure of the system remain steadily high despite changes in the operating temperature.

Recommendation: It should be noted that failure of the MOSFETs account for more than three quarters of the failure of the SBC system regardless of which type of failure scenario is being investigated. According to [13], the main reason MOSFETs fail is due to Electrical Overstress (EOS) which includes Unclamped Inductive Switching (UIS), linear mode operation during switching, and over current. A common outcome is the melting of the die and metal due to burning. To improve the reliability of the system it is essential to design circuits that protect the MOSFET, including using Schottky diode in series with the MOSFET and a fast recovery diode in parallel, and improving switching control by making use of dead time between switching transitions. However, adding lots of protective and redundant features into a PCB leads to cost increases, that must be balanced against application requirements. The field test of the SBC during sea trials remarkably shows no failures to date. However, not enough time has elapsed to make a valid judgement for system reliability. Furthermore, the system was operated in ambient temperatures below 45°C, thus it has better reliability practically than in simulation. In the absence of testbeds that can conduct accelerated stress tests, years of sea trials will be needed before a judgement can be made as to whether the SBC components tend towards short or open circuit failure.

V. Conclusion

This paper has presented a model to describe the overall reliability of the SBC system used for the battery charging controller in a fishing trawler. The reliability model has been developed for two common types of component failure categories using series and parallel association. Simulation results have demonstrated that the studied system has a MTBF of between 5 to 11 years under the worst-case scenario; however, practical data is not enough yet to compare with simulation data and determine whether the SBC components tends to fail as open circuit or short circuit conditions.

Acknowledgement

Authors acknowledge Flanders make for the support to this research group.

References

[1] Yang, Y., Wang, H., Sangwongwanich, A., Blaabjerg, F., “Power Electronics Handbook”, Fourth edition, (2018), Chapter 45, pp. 1423-1440.

[2] Kales, P., Reliability for Technology, Engineering and Management. Prentice-Hall, 1998. pp. 7-13.

[3] Silverman, M., Kleynar, A., “What is Design for Reliability and What it is Not”, DOI: 10.1109/RAMS.2012.6175520, (2012).

[4] O’Connor, P., “Practical Reliability Engineering”. John Wiley and Sons, 2002, pp. 414-452.

[5] Chakraborty, S., Safayet, U. S. M., Razzak, M. A., “Quantifying Solar Potential on roof Surface Area of Fishing Trawlers in Chittagong Region in Bangladesh”, in proc. 2016 IEEE Innovative Smart Grid Technologies - Asia (ISGT-Asia), 2016, pages: 833-837.

[6] Chakraborty, S., Hasan, M. M., Worighi. I., Hegazy, O., Razzak, M. A., “Performance Evaluation of a PID-Controlled Synchronous Buck Converter based Battery Charging Controller for Solar Powered Lighting System in a Fishing Trawler”, Energies, MDPI, 2018, 11, 2722.

[7] Depew, J., Mosfet, L. “Efficiency Analysis of a Synchronous Buck Converter using Microsoft Office Excel-Based Loss Calculator.” In *Appl. Note*; Microchip Technology Inc.: Chandler, AZ, USA, 2012; pp. 1–14.

[8] Chakraborty, S., Vu, H. N., Hasan, M. M., Tran, D-D., El Baghdadi, M., & Hegazy, O. “DC-DC Converter Topologies for Electric Vehicles, Plug-in Hybrid Electric Vehicles and Fast Charging Stations: State of the Art and Future Trends.” Energies, 12(8), [1569].

[9] Metglas Datasheet: http://elnamagnetics.com/wp-content/uploads/catalogs/Metglas/powerlite.pdf, accessed on 20 Oct. 2018.

[10] Military Handbook MIL HDBK 217F: Reliability Prediction of Electronic Equipment. USA Department of Defense. Washington, USA, 1991. December. Available at http://snebulos.mit.edu/projects/reference/MIL-STD/MIL-HDBK-217F-Notice2.pdf.

[11] Richardeau, F., Pham, T. T. L., “Reliability Calculation of Multilevel Converters: Theory and Applications”, IEEE Transaction on Industrial Electronics, 60(10), 2013.

[12] Tu, P., Wang, P., Yang, S., “Reliability and Cost based Redundancy Design for Modular Multilevel Converter”, IEEE Transaction on Industrial Electronics, 2018, DOI: 10.1109/TIE.2018.2793263

[13] Nel, B. J., Perinpanayagam, S., “A Brief Overview of SiC MOSFET Failure Modes and Design Reliability”, 5th International Conference on Through-life Engineering Service (TESConf 2016), pp 280 – 285.